Article ID: 1000-324X(2023)02-0219-06 **DOI:** 10.15541/jim20220300

Irradiation Damage of CaF_2 with Different Yttrium Concentrations under 193 nm Laser

WANG Huajin[1,2], KOU Huamin[2], WANG Yongzhe[2], JIANG Dapeng[2], ZHANG Bo[2], QIAN Xiaobo[2], WANG Jingya[2], ZHU Linling[4], ZENG Aijun[4], YANG Qiuhong[1], SU Liangbi[2,3]

(1. School of Materials Science and Engineering, Shanghai University, Shanghai 200444, China; 2. State Key Laboratory of High Performance Ceramics and Superfine Microstructure, Shanghai Institute of Ceramics, Chinese Academy of Sciences, Shanghai 201899, China; 3. Center of Materials Science and Optoelectronics Engineering, University of Chinese Academy of Sciences, Beijing 100049, China; 4. Shanghai Institute of Optics and Fine Mechanics, Shanghai 201800, China)

Abstract: Radiation resistance of CaF_2 crystal is one of the critical properties in the application of deep ultraviolet lithography, but the damage process under 193 nm laser irradiation is still unclear. This paper reports the damage behavior of CaF_2 crystals under 193 nm laser irradiation and the key defect factors affecting the damage. Through the 193 nm laser irradiation experiment, it is found that the crystal damage is mainly manifested as the radiation-induced color centers inside the crystal and the radiation-induced damage pits on the surface. Irradiation-induced color centers were analyzed by UV-visible spectrophotometer, and linear fitting was performed between absorption coefficients of different color centers and Y impurity contents. The results show that Y ion has a low-order orbit that overlaps with the F center structure wave function, and hybridizes to form a stable structure. There is a linear relationship between Y ions contents and intrinsic color centers of CaF_2 crystals, confirming that Y element is the key impurity ion affecting the formation of color centers. Energy dispersive X-ray spectrometer (EDS) results show that the content of calcium in the damage pits increases and the content of fluorine decreases, which confirms that the diffusion of H centers and the aggregation of F centers lead to irradiation damage. Electron backscatter diffraction (EBSD) results show that surface irradiation damage occurs preferentially at dislocations. Therefore, reducing the impurity content and dislocation density is an important way to improve the anti-irradiation damage performance of calcium fluoride crystals under 193 nm laser.

Key words: CaF_2 crystal; color center; laser irradiation damage; impurity content; dislocation density

CaF_2 has high transparency in the range from 130 nm to 9 μm and is widely used in deep ultraviolet (DUV) to far infrared (IR) optical components. It is even more irreplaceable in applications in the extreme UV edge. The most demanding application for CaF_2 is DUV optical microlithography, where CaF_2 is a crucial lens material. Although the transmittance of CaF_2 crystal meets the 193 nm lithography requirements, even when the laser energy density is below the damage threshold, they cannot avoid the optical damage caused by cumulative ultraviolet radiation. This behavior is known as the incubation effect[1-4]. To improve the resistance of CaF_2 to DUV laser irradiation, investigating the interaction between the DUV laser and CaF_2 and clarifying the mechanism of laser damage is very important.

After irradiation with a 193 nm laser, high-quality CaF_2 still show coloration effects to some extent. The investigation of these coloration effects, the so-called laser damage, has been studied intensively in recent years[5-9]. The coloration of fluorite (natural CaF_2) was studied widely. Smakula, *et al*[10-12] obtained the coloring effect of calcium fluoride by X-ray, γ-ray, neutron irradiation, and electron irradiation respectively. According to Mie's theory[13-15], the coloration effects were due to

Received date: 2022-05-27; **Revised date:** 2022-06-04; **Published online:** 2022-08-26
Foundation item: Strategic Priority Program of the Chinese Academy of Sciences (XDA25020313); National Natural Science Foundation of China (61925508); Science and Technology Commission of Shanghai Municipality (20501110300, 20511107400); CAS Project for Young Scientists in Basic Research (YSBR-024)
Biography: WANG Huajin (1996–), male, Master candidate. E-mail: wanghuajin@shu.edu.cn
王华进(1996–), 男, 硕士研究生. E-mail: wanghuajin@shu.edu.cn
Corresponding author: KOU Huamin, associate professor. E-mail: huaminkou@mail.sic.ac.cn; SU Liangbi, professor. E-mail: suliangbi@mail.sic.ac.cn
寇华敏, 高级工程师. E-mail: huaminkou@mail.sic.ac.cn; 苏良碧, 研究员. E-mail: suliangbi@mail.sic.ac.cn

the formation of colloidal particles in the mineral. Besides, Przibram[16] showed that many coloration effects could be associated with impurity ions, especially rare-earth ions. Bill and coworkers[17-18] extensively studied the coloration of natural fluorite and doped CaF_2 with many impurity ions. Alig, *et al*[19-20] believed that the orbital hybridization of impurity ions such as Y, La, Ce, Gd, Tb, and Lu with intrinsic defects resulted in color center absorption. Among the impurity ions, the Y ion was the main impurity element, Y is easily incorporated into CaF_2 lattice due to very similar ionic radius and chemical properties to Ca. Mizuguchi and coworkers[21] have shown that the damage resistance of CaF_2 crystals doped with only 5 μg/g of Y decreased strongly comparing to pure CaF_2 crystals (Y content 1 μg/g). All these studies show that impurity ions promote the formation of calcium colloids. However, the growth behavior of calcium colloids in crystals is still unclear. In this study, CaF_2 crystals with different Y impurity content were fabricated to study the radiation-induced color centers, and the relationship between Y impurity contents and different color centers was investigated. The formation and growth behavior of calcium colloids were also analyzed combining the EDS, EBSD and morphologies analysis in the damage area. The damage process and mechanism under 193 nm laser irradiation were proposed, which was of great significance to improve the calcium fluoride crystal damage performance.

1 Experimental

1.1 Sample preparation and materials properties

The CaF_2 crystals used in the experiment were grown by vertical Bridgman method. The raw materials were high-purity CaF_2 with different Y impurity contents. Appropriate PbF_2 were added as an oxygen scavenger. The furnace used was vacuum-tight and the maintained pressure was below 5×10^{-3} Pa during the entire progress of crystal growth. Crystals were oriented using X-ray diffraction methods and cut perpendicular to the (111) axis. Each sample was cut into a circular piece with 25 mm in diameter and 4 mm in thickness. Samples were both ends polished for optical transmission measurements and other experiments.

The actual concentration of Y ions in these samples was measured by inductively coupled plasma mass spectroscopy (ICP-MS). UV-VIS-NIR spectrophotometer was used to measure the optical absorption spectra. Scanning electron microscope (SEM, FEI Magellan 400) was used to characterize the structure of subsurface damaged regions. Energy dispersive X-ray spectroscope (EDS, Oxford X-MAX80) and electron backscatter diffraction (EBSD, Oxford NordlysNano), integrated in the SEM were used to characterize elements and structure on top and below the damaged mirror surface to clarify the chemical modification of the bulk material. All measurements mentioned above were carried out at room temperature. Etch pits were obtained by etching the cleaved surface of sample in HCl aqueous solution at 60 ℃ for about 10 min. The etched samples were photographed under an optical microscope with a magnification of 63 times to obtain the etched morphology.

The morphology and absorption spectrum of the samples before irradiation are shown in Fig. 1. The yttrium impurity ion content of sample 1# is 0.47 μg/g, and the values for sample 2# and sample 3# are 1.60, 5.74 μg/g respectively. The content of other impurity cations is less than 0.01 μg/g. The samples are numbered as 1#–3# according to the Y content.

1.2 Laser damage experiment

The samples were exposed to UV light with a solid-state pulse power switch from an argon fluoride excimer laser (ArF, 193 nm, MLI-FBG). Damage experiments used a square beam profile (3 mm×3 mm, 106 $(mJ\cdot cm^{-2})$/pulse). The frequency was fixed to 800 Hz.

According to ISO 21254 laser damage test method, the laser damage tests were carried out in the mode S-on-1, and the number of pulses expresses the radiation resistance of crystals.

2 Results and discussion

2.1 Irradiation-induced color centers analysis

Laser radiation damage is characterized by a loss of transmittance of the material due to the formation of absorption and scattering centers. The radiation damage resistance of the crystal is expressed as the number of pulses at which transmittance loss is observed. The typical morphologies of the laser-induced damage are shown in Fig. 2(a), obvious black shading was found in the crystal.

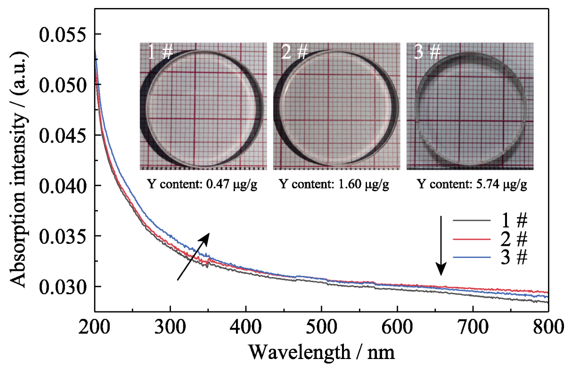

Fig. 1 Absorption spectra and morphologies of samples before irradiation

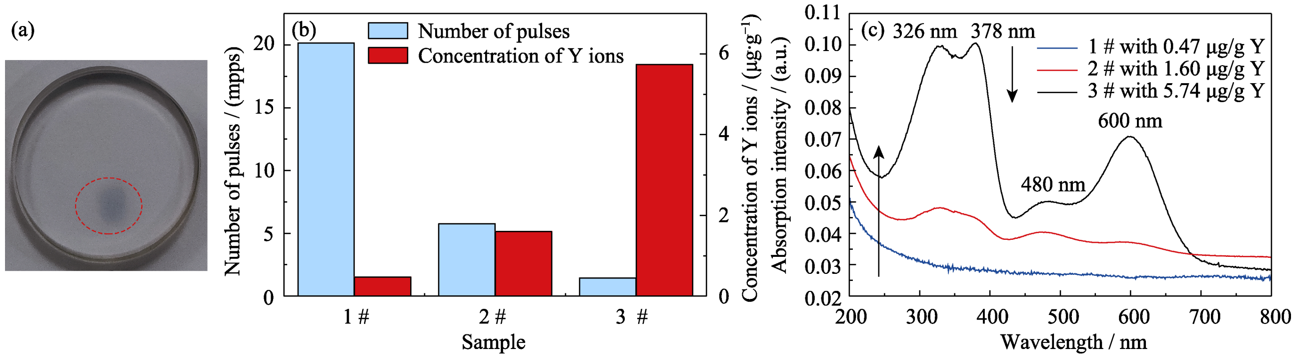

Fig. 2 Radiation damage result

(a) Damage morphology; (b) Relationship between Y ions and radiation resistance; (c) Damaged region absorption spectra

mpps: million pulsesper second

The results of the laser damage experiment are shown in Fig. 2(b). With the increase of Y ions concentration, the radiation damage resistance of the crystal decreased significantly.

The absorption spectra of the samples after irradiation are shown in Fig. 2(c). There are four obvious absorption bands located at 326, 378, 480, and 600 nm, respectively. This spectrum is similar to the absorption spectrum of the color center induced by X-ray and high-energy electron irradiation[22-26]. The absorption around 326 nm was aroused by the formation of H center (a fluorine atom at an interstitial site covalently bound to a lattice anion), while 378 nm band belongs to the F center absorption (an electron trapped at an anion vacancy). The absorption peak at about 600 nm is considered to be caused by the M center (M centers are two adjacent F centers). The absorption peak at 480 nm is mainly due to the oxygen incorporated into the lattice[26].

Referring to the color center structure and performance, the loss of crystal transmittance can be summarized as the following process.

Generation of electron hole pairs:

$$0 \overset{\text{Irradiation}}{\Leftrightarrow} e' + h^{\bullet} \tag{1}$$

Generation of Frenkel defects:

$$0 \overset{\text{Irradiation}}{\Leftrightarrow} F_i' + V_F^{\bullet} \tag{2}$$

Anion vacancies capture electrons to form F center:

$$V_F^{\bullet} + e' \overset{\text{Irradiation}}{\Leftrightarrow} [V_F^{\bullet} + e'] \tag{3}$$

Reversible conversion process (F center and M center):

$$2[V_F^{\bullet} + e'] \overset{\text{Thermal}}{\Leftrightarrow} [V_F^{\bullet} + e']_2 \tag{4}$$

The formation process of color centers are shown in Fig. 3(a). Under the 193 nm laser irradiation, electrons were excited to the conduction band through a two-photon absorption process as show in Eq. (1), producing self-trapped excitons (STE). STE is a kind of metastable defect that can release energy and transform into a pair of F (Eq. (2) and Eq. (3)) and H centers[27]. Since the yttrium ions has low-lying s and d valence orbitals which overlap the F-center wave functions. Orbital hybridization as shown in Fig. 3(b) occurs[21], leads to the emergence of color center absorption peaks. In addition, since the F center has a more robust localized structure and symmetry than the H center, the diffusion energy barrier of the F center is much higher than that of the H center in the CaF_2 crystal[6]. These characteristics lead to a gradual increase of the F center in the irradiated area during the

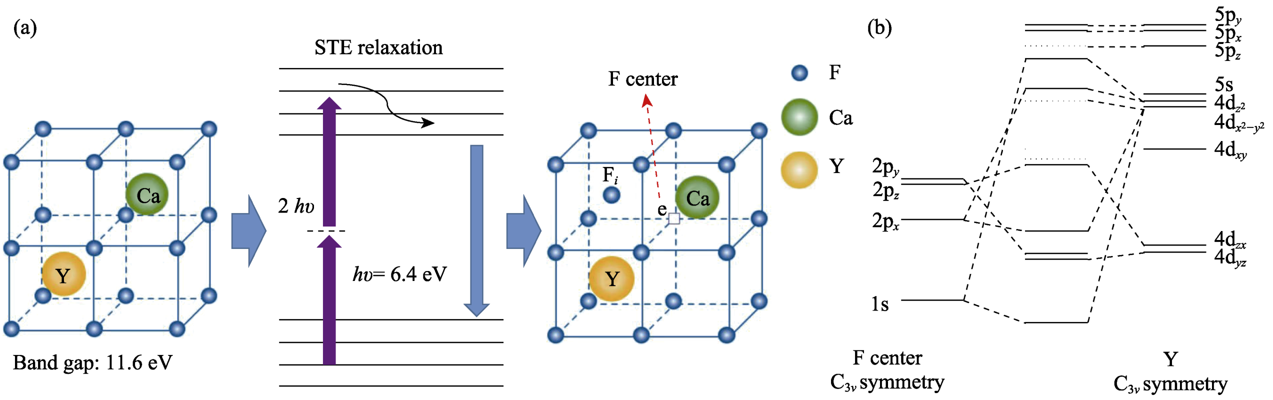

Fig. 3 Schematic diagrams of the formation process of color centers

(a) F center generated by self-excited defects formed by two-photon absorption; (b) defect-impurity orbital energy levels of the YFC irradiation process. The F centers gradually gather into M center (Eq. (4)) and other F center clusters. The creation of M centers indicates the beginning of the calcium colloid generation. During the long-term irradiation, the F center clusters aggregate to form stable calcium colloids, which is responsible for the black shading shown in Fig. 2(a). Calcium colloids results in absorption and scattering, significantly decreasing the crystals' transparency.

In the process of irradiation damage, impurity ions reduce the F-H pair formation energy and stabilize the F center and H center. This behavior has been confirmed by various experimental data and calculation results[3, 5, 11, 13]. In order to understand accurately the effect of Y ions on the damage during irradiation, the absorption coefficient was used in this work to assess the damage degree. The linear fitting results of different color center absorption bands are shown in Fig. 4. The slopes of the fitted curves at 326 nm (H center) and 378 nm (F center) are extremely similar, indicating that these two color centers increase synchronously with the increase of Y ion content during the irradiation process. H center appeared once F center are generated, which is a typical Frenkel defect (Eq. (2)). During the irradiation process, STE directly produces F-H pairs to form H and F centers, and M centers are formed by the aggregation of F centers, so the fitted curve at 600 nm (M center) also has a linear relationship with the Y ion content, but its slope is much smaller than that at 326 and 378 nm. The linear fitting results indicate that Y element is the key impurity in the formation of crystal intrinsic defects (F, H and M centers). No good linear fitting results were obtained at 480 nm, indicating that the color center at 480 nm was not dominated by the content of Y ions.

2.2 Damage pits analysis

The damage pits shown in Fig. 5 was found by observing the damaged area with the electron microscope. Fig. 5(a) is the morphology of the damage pits in the irradiation area. Fig. 5(b) is the damage pits clustered together after further magnification. The morphology is similar to the melting damage, and there are small granular substances in the damaged area. Fig. 5(c) shows a single damage pit, which is triangular in shape, and there are three black lines (marked with white dashed circle) approximately 120° in the middle of the pit. This morphology is consistent with the dislocation etch pits obtained by HCl corrosion in Fig. 5(d), but the side length of the damaged pits is only 10 μm, which is 1/4 of the etch pits. This phenomenon indicates that the melting damage may occur centered on dislocations.

To clarify the distribution of damage craters, the damaged areas of the crystals using electron backscatter diffraction (EBSD) were analyzed. The result is shown in Fig. 6. Secondary electron imaging is shown in Fig. 6(a),

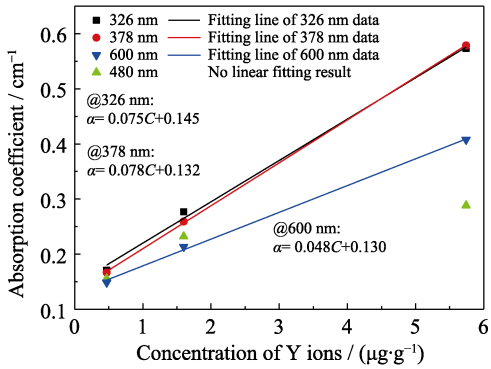

Fig. 4 Linear fitting of color center absorption coefficient and Y ion concentration

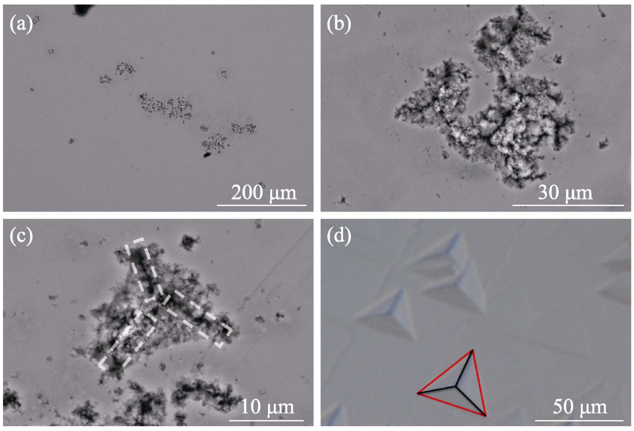

Fig. 5 SEM images of damaged area
(a) Complete morphology of the damage pits; (b) Aggregate damage pits; (c) Single damage pit; (d) Etch pits of dislocations (HCl etching)

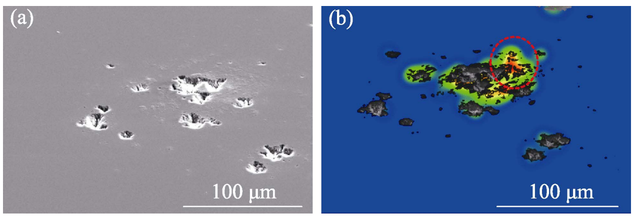

Fig. 6 Damage morphologies of sample 2# under different modes of SEM
(a) Secondary electron image; (b) Stress distribution diagram, blue, green and red regions indicate the variation of stress from low to high, respectively

and the triangle shape of the damage pits is consistent with the crystal dislocation etch pit in Fig. 5(d). Moreover, the Kernel average misorientation (KAM) distribution was calculated to demonstrate the stress distribution, and the different colors represent different stress states at the corresponding areas, as shown in Fig. 6(b). In this figure, blue, green and red regions indicate the variation of stress from low to high, respectively. Obvious stress distribution can be detected near the damage pits, as shown by the green and red regions. No diffraction pattern was recorded in the dark region, indicating the crystal structure here was damaged basically. In addition to the triangular shape of the crystal damage pit, triangular stress distribution also appeared in the undamaged area (marked by the red dotted circle). This is due to the mismatch structure between calcium colloid induced by damage and calcium fluoride matrix. Since calcium colloids are mainly composed of calcium atoms, their properties are considered to be similar to metallic calcium.

As shown in Table 1, the lattice constant of CaF_2 is 2% smaller than that of metallic Ca. Since the elastic stiffness constants of CaF_2 is about an order of magnitude higher than that of metallic Ca, the stress is absorbed by the Ca colloid with a smaller elastic stiffness constant. In Fig. 6(b), the calcium colloid absorbs the stress in a triangular shape, which confirms that the calcium colloid tends to grow at lattice defects, such as dislocations, small-angle grain boundaries, *etc*.

As mentioned in Section 3.1, the diffusion velocity of the H centers in the irradiation area is greater than that of the F centers, which is confirmed by EDS analysis of the damage pit area as shown in Fig. 7. The results show that the relative content of calcium increases sharply, and the relative content of F decreases sharply in the damaged area. We propose the following mechanism for the damage process: due to the higher diffusion velocity of H center than F center, a large number of F centers are left in the irradiation area and gradually aggregate into F center aggregates such as M centers, and finally grow into the calcium colloid. With the increase of the number of pulses, the calcium colloid continuously absorbs the laser energy, reaching the melting point, which leads to the damage of the crystal surface. The melting point of calcium is 842 ℃, and the melting point of CaF_2 crystal is 1423 ℃. With the formation of calcium colloids, the crystal is more prone to melting damage.

Table 1 Elastic stiffness constants c_{ij} and lattice constant of Ca and CaF_2[28-29]

Crystal	c_{11}/GPa	c_{12}/GPa	Lattice constant/nm
CaF_2	165	46	0.546
Ca	16	8	0.558

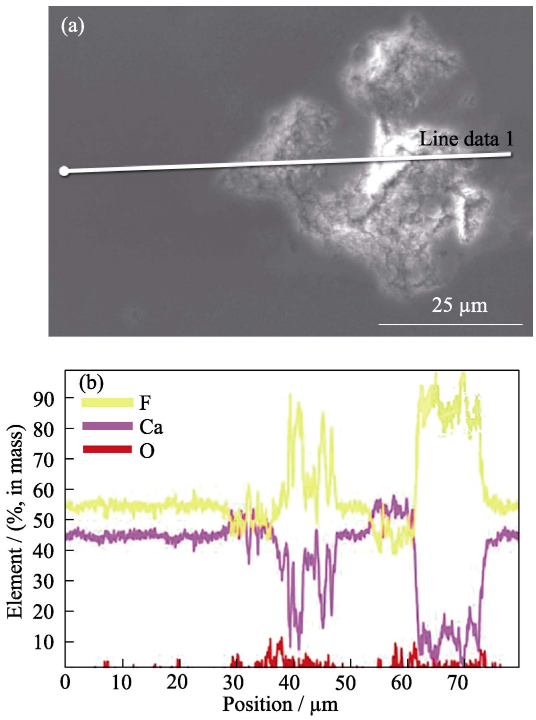

Fig. 7 EDS analysis of sample 2# damage pits

(a) EDS sampling location; (b) EDS results of elements at different positions

Colorful figure is available on website

3 Conclusions

We investigated the laser damage of CaF_2 crystals with different contents of Y ions. Under the irradiation of a 193 nm ultraviolet laser beam with an energy density of 106 mJ/cm^2, Y ions promotes the formation of F-H pairs and reduces the radiation resistance of the crystal. The EDS analysis of the damage pits confirmed that the damage process of the CaF_2 under 193 nm laser irradiation started from F centers aggregation and the formation of the calcium colloid. Furthermore, the EBSD analysis of the damage area shows that the calcium colloid grown along the dislocation. It is essential to reduce the impurity content and dislocation density for improving the radiation damage resistance of CaF_2 crystals under 193 nm laser.

References:

[1] KAWAGUCHI Y, DAWES M L, LANGFORD S C, *et al*. Interaction of wide band gap single crystals with 248 nm excimer laser irradiation. VII. Localized plasma formation on NaCl single crystal surfaces. *Journal of Applied Physics*, 2001, **89(4):** 2370.

[2] REIF J, PETZOLDT S, ELG A P, *et al*. The role of defects in laser surface damage thresholds of fluoride crystals. *Applied Physics A*, 1989, **49(2):** 199.

[3] REICHLING M, SILS J, JOHANSEN H, *et al*. Nanosecond UV laser damage and ablation from fluoride crystals polished by different techniques. *Applied Physics A*, 1999, **69(1):** S743.

[4] JOHANSEN H, GOGOLL S, STENZEL E, *et al*. Sem-analysis of fracture features formed in excimer-laser induced surface damage of CaF_2. *Radiation Effects and Defects in Solids*, 1995, **136(1–4):** 151.

[5] MUEHLIG C, TRIEBEL W, TOEPFER G, *et al*. Laser-induced fluorescence of calcium fluoride at 193 and 157 nm excitation. *SPIE*, 2003, **5188:** 123.

[6] RIX S, NATURA U, LETZ M, *et al*. A microscopic model for long-term laser damage in calcium fluoride. *International Society for Optics and Photonics*, 2009, **7504:** 75040J.

[7] KOMINE N, SAKUMA S, SHIOZAWA M, *et al*. Influence of sodium impurities on ArF excimer-laser-induced absorption in CaF_2 crystals. *Applied Optics*, 2000, **39(22):**3925.

[8] BAUER M, BISCHOFF M, JUKRESCH S, *et al*. Exterior surface damage of calcium fluoride outcoupling mirrors for DUV lasers.

Optics Express, 2009, **17(10):** 8253.

[9] AZUMI M, NAKAHATA E. Laser damage of calcium fluoride by ArF excimer laser irradiation. *SPIE*, 2015, **9632:** 199.

[10] IZERROUKEN M, GUERBOUS L, MEFTAH A. Colour centres formation in CaF_2 single crystals by γ-rays and reactor neutrons. *Nuclear Instruments and Methods in Physics Research Section A: Accelerators, Spectrometers, Detectors and Associated Equipment*, 2010, **621(1/2/3):** 68.

[11] SMAKULA A. Color centers in calcium fluoride and barium fluoride crystals. *Physical Review*, 1950, **77(3):** 408.

[12] SCOULER W J, SMAKULA A. Coloration of pure and doped calcium fluoride crystals at 20 ℃ and –190 ℃. *Physical Review*, 1960, **120(4):** 1154.

[13] MIE G. Beiträge zur optik trüber medien, speziell kolloidaler metallösungen. *Annalen der physik*, 1908, **330(3):** 377–445.

[14] BEUNEU F, FLOREA C, VAJDA P. EPR-study of electron-radiation induced Ca colloids in CaF_2 crystals. *Radiation Effects and Defects in Solids*, 1995, **136(1–4):** 175.

[15] BATOOL A, IZERROUKEN M, AISIDA S O, *et al*. Effect of Ca colloids on *in-situ* ionoluminescence of CaF_2 single crystals. *Nuclear Instruments and Methods in Physics Research Section B: Beam Interactions with Materials and Atoms*, 2020, **476:** 40.

[16] PRZIBRAM K. Absorption bands and electron transitions in coloured fluorites. *Nature*, 1938, **141(3578):** 970.

[17] BILL H, LACROIX R. EPR of a centre in Y^{3+} doped artificial CaF_2 crystals. *Physics Letters*, 1966, **22(3):** 250.

[18] BILL H. Endor investigation of Gd^{3+} in CaF_2 crystals. *Physics Letters A*, 1969, **29(10):** 593.

[19] ALIG R C. Theory of photochromic centers in CaF_2. *Physical Review B*, 1971, **3(2):** 536.

[20] STAEBLER D L, SCHNATTERLY S E. Optical studies of a photochromic color center in rare-earth-doped CaF_2. *Physical Review B*, 1971, **3(2):** 516.

[21] MIZUGUCHI M, HOSONO H, KAWAZOE H, *et al*. Generation of optical absorption bands in CaF_2 single crystals by ArF excimer laser irradiation: effect of yttrium impurity. *Journal of Vacuum Science & Technology A: Vacuum, Surfaces, and Films*, 1998, **16(5):** 3052.

[22] PARKER S, SONG K S, CATLOW C R A, *et al*. Geometry and charge distribution of H centres in the fluorite structure. *Journal of Physics C: Solid State Physics*, 1981, **14(28):** 4009.

[23] KAMIKAWA T, KAZUMATA Y, KIKUCHI A, *et al*. The F center in calcium fluoride. *Physics Letters*, 1966, **21(2):** 126.

[24] HAYES W. Point defects in alkaline earth fluorides. *Radiation Effects*, 1970, **4(2):** 239.

[25] MA Y, ROHLFING M. Optical excitation of deep defect levels in insulators within many-body perturbation theory: the F center in calcium fluoride. *Physical Review B*, 2008, **77(11):** 115118.

[26] RAUCH R, SCHWOTZER G. Disturbed colour centres in oxygen- and alkali-doped alkaline earth fluoride crystals after X-ray irradiation at 77 and 295 K. *Physica Status Solidi (a)*, 1982, **74(1):** 123.

[27] TANIMURA K. Femtosecond time-resolved spectroscopy of the formation of self-trapped excitons in CaF_2. *Physical Review B*, 2001, **63(18):** 184303.

[28] SHANG S L, SAENGDEEJING A, MEI Z G, *et al*. First-principles calculations of pure elements: equations of state and elastic stiffness constants. *Computational Materials Science*, 2010, **48(4):** 8136.

[29] GUO Y, FANG Y, LI J. Detailed structural, mechanical, and electronic study of five structures for CaF_2 under high pressure. *Chinese Physics B*, 2021, **30(3):** 030502

193 nm 激光下不同含量 Y 杂质 CaF_2 晶体辐照损伤研究

王华进[1,2], 寇华敏[2], 王墉哲[2], 姜大朋[2], 张 博[2], 钱小波[2],
王静雅[2], 朱琳玲[4], 曾爱军[4], 杨秋红[1], 苏良碧[2,3]

(1. 上海大学 材料科学与工程学院, 上海 200444; 2. 中国科学院 上海硅酸盐研究所, 透明光功能无机材料重点实验室, 上海 201899; 3. 中国科学院大学 材料科学与光电工程中心, 北京 100049; 4. 中国科学院 上海光学精密机械研究所, 上海 201800)

摘 要: 氟化钙晶体的抗辐照性能是其在深紫外光刻应用中的关键性能之一, 目前氟化钙晶体在 193 nm 激光辐照下的损伤过程尚不清楚。本文报道了 193 nm 激光辐照下氟化钙晶体的损伤行为及影响损伤的关键缺陷因素。通过 193 nm 激光辐照试验, 发现晶体损伤主要表现为晶体内部产生的辐照诱导色心与表面产生的辐照诱导损伤坑。通过紫外–可见分光光度计对辐照诱导色心分析, 并将不同色心吸收系数与 Y 杂质含量进行线性拟合。结果表明: Y 离子具有与 F 心结构波函数发生重叠的低位轨道, 两者发生轨道杂化易形成色心稳定结构; 线性拟合结果表明 Y 离子含量与氟化钙晶体本征色心之间存在线性关系, 说明 Y 元素是影响色心形成的关键杂质离子。实验表征了辐照诱导损伤坑的元素分布和结构缺陷。EDS 结果表明损伤坑处伴随着钙元素含量上升和氟元素含量下降, 证实 H 心扩散、F 心聚集导致了辐照损伤; EBSD 结果表明表面辐照损伤优先在位错处产生。因此, 降低杂质含量及位错密度是提高氟化钙晶体在 193 nm 激光下抗辐照损伤性能的重要途径。

关 键 词: 氟化钙晶体; 色心; 激光辐照损伤；杂质含量; 位错密度

中图分类号: TQ174 **文献标志码:** A